JOURNAL OF GEOPHYSICAL RESEARCH: BIOGEOSCIENCES, VOL. 118, 1–17, doi:10.1002/jgrg.20039, 2013

Forecasting net ecosystem CO_2 exchange in a subalpine forest using model data assimilation combined with simulated climate and weather generation

Laura E. Scott-Denton,[1] David J.P. Moore,[2] Nan A. Rosenbloom,[3] Timothy G.F. Kittel,[4] Sean P. Burns,[3,5] David S. Schimel,[6] and Russell K. Monson[1,2,7]

Received 25 September 2012; revised 4 February 2013; accepted 8 February 2013.

[1] Forecasting the carbon uptake potential of terrestrial ecosystems in the face of future climate change has proven challenging. Process models, which have been increasingly used to study ecosystem-atmosphere carbon and water exchanges when conditioned with tower-based eddy covariance data, have the potential to inform us about biogeochemical processes in future climate regimes, but only if we can reconcile the spatial and temporal scales used for observed fluxes and projected climate. Here, we used weather generator and ecosystem process models conditioned on observed weather dynamics and carbon/water fluxes, and embedded them within climate projections from a suite of six Earth Systems Models. Using this combination of models, we studied carbon cycle processes in a subalpine forest within the context of future (2080–2099) climate regimes. The assimilation of daily averaged, observed net ecosystem CO_2 exchange (NEE) and evapotranspiration (ET) into the ecosystem process model resulted in retrieval of projected NEE with a level of accuracy that was similar to that following the assimilation of half-daily averaged observations; the assimilation of 30 min averaged fluxes or monthly averaged fluxes caused degradation in the model's capacity to accurately simulate seasonal patterns in observed NEE. Using daily averaged flux data with daily averaged weather data projected for the period 2080–2099, we predicted greater forest net CO_2 uptake in response to a lengthening of the growing season. These results contradict our previous observations of reduced CO_2 uptake in response to longer growing seasons in the current (1999–2008) climate regime. The difference between these analyses is due to a projected increase in the frequency of rain versus snow during warmer winters of the future. Our results demonstrate the sensitivity of modeled processes to local variation in meteorology, which is often left unresolved in traditional approaches to earth systems modeling, and the importance of maintaining similarity in the timescales used in ecosystem process models driven by downscaled climate projections.

Citation: Scott-Denton, L. E., D. J. P. Moore, N. A. Rosenbloom, T. G. F. Kittel, S. P. Burns, D. S. Schimel, and R. K. Monson (2013), Forecasting net ecosystem CO_2 exchange in a subalpine forest using model data assimilation combined with simulated climate and weather generation, *J. Geophys. Res. Biogeosci.*, *118*, doi:10.1002/jgrg.20039.

1. Introduction

[2] The uptake of atmospheric CO_2 by forest ecosystems is the largest and most persistent component of the terrestrial global carbon sink [*Pan et al.*, 2011]. Forest inventory data, remotely sensed satellite images, and computer models have provided evidence that regional forest carbon sinks are weakening, and some studies have shown that this weakening is due to changes in climate and associated effects on physiological processes in plants and soils [*Canadell et al.*, 2007; *Zhao and Running*, 2010; *Gurney and Eckels*, 2011]. Other studies have provided evidence that sinks have not weakened in their overall strength but that they have become more variable in their interannual responses to climate variation [*Knorr*, 2009; *Gloor et al.*, 2010; *Ballantyne et al.*, 2012]. Accurate forecasts of climate change and its effect on carbon sinks cannot be made without an understanding of the coupling between forest metabolism and specific climate

Additional supporting information may be found in the online version of this article.

[1]Department of Ecology and Evolutionary Biology, University of Colorado, Boulder, Colorado, USA.
[2]School of Natural Resources and the Environment, University of Arizona, Tucson, Arizona, USA.
[3]National Center for Atmospheric Research, Boulder, Colorado, USA.
[4]Institute of Arctic and Alpine Research, University of Colorado, Boulder, Colorado, USA.
[5]Department of Geography, University of Colorado, Boulder, Colorado, USA.
[6]Jet Propulsion Laboratory, California Institute of Technology, Pasadena, California, USA.
[7]Laboratory for Tree Ring Research, University of Arizona, Tucson, Arizona, USA.

Corresponding author: L. E. Scott-Denton, Department of Ecology and Evolutionary Biology, University of Colorado, Boulder, CO 80309, USA. (laura_ontheweb@yahoo.com)

2169-8953/13/10.1002/jgrg.20039

variables, and in particular, the role of nonlinear responses as metabolic processes respond to climate change [*IPCC*, 2007]. In fact, it is the nonlinear responses in both the first-order and higher order interactions with climate that have proven to be the most difficult aspects of future climate projections [*Meir et al.*, 2006; *Heimann and Reichstein*, 2008; *Friedlingstein and Prentice*, 2010; *Milcu et al.*, 2012]. For example, *Medvigy et al.* [2010] found that the nonlinearities that characterize the physiological responses of processes such as photosynthesis, respiration, and transpiration to variable climate can have large effects on projections of regional carbon balance, and these responses are often missed in the coarse spatiotemporal resolution used in global Earth Systems Models (ESMs).

[3] The coupling between forest carbon exchange processes and systematic changes in future climate can be explored through existing ESMs [*Moss et al.*, 2010; *Taylor et al.*, 2012]. When fully coupled to global climate simulation, land surface processes are simulated at relatively short time steps (subhourly-to-hourly) [e.g., *Washington and Meehl*, 1984; *Oleson et al.*, 2008], but results are rarely analyzed at these shorter timescales. Rather, the results of such simulations are assessed across months or multiple decades, or they are used to establish future steady states of the earth system at a defined endpoint [e.g., *Booth et al.*, 2011]. In order to explore process-climate interactions in more nuanced scenarios, the components of land surface models are often developed and run "offline," where they can be parameterized and validated using observations of a more restricted spatiotemporal scope, and then reinserted into ESMs to project future states of the entire global system [e.g., *Thornton and Zimmerman*, 2007; *Lawrence et al.*, 2007]. Recently, a new generation of ecosystem process models has emerged, which are intended specifically for use with tower flux networks that have generated observations of ecosystem-atmosphere carbon and water fluxes for a decade or longer [e.g., *Stöckli et al.*, 2008; *Williams et al.*, 2009]. These models have been deployed as a means of assessing seasonal and interannual controls over the photosynthetic and respiratory fluxes within a single ecosystem [e.g., *Braswell et al.*, 2005; *Sacks et al.*, 2006, 2007] or in ecosystems and biomes extending across climate gradients [e.g., *Schwalm et al.*, 2010; *Richardson et al.*, 2012]. Most often, models of this type have been used for the purpose of inverse parameter estimation, including the partitioning of observed net ecosystem CO_2 exchange (NEE) into estimates of its component photosynthetic and respiratory processes [e.g., *Stoy et al.*, 2005; *Fox et al.*, 2009; *Richardson et al.*, 2010; *Schwalm et al.*, 2010; *Dietze et al.*, 2011; *Schaefer et al.*, 2012]. These types of models have not yet been implemented in fully coupled ESMs; but when properly used for parameter estimation, they provide the potential to explore the response of ecosystem-atmosphere carbon fluxes to future climate change [*Keenan et al.*, 2012].

[4] The process of posterior parameter estimation is a type of inverse modeling—observations from a flux time series are assimilated into the model and compared to model projections of the flux following iterative adjustments in parameter values. After numerous iterations, the parameter set that produces the least error between observations and projections is considered "most parsimonious." Often, several alternative sets of parameters will provide similarly low levels of error, thus permitting one to estimate "allowed variance" for each optimized parameter [*Braswell et al.*, 2005]. Once parameter values have been optimized through this inverse process, the model can be run in forward mode to predict fluxes given a prescribed set of meteorological drivers; this approach improves accuracy of model prognosis at temporal scales that match those of the assimilated data [*Braswell et al.*, 2005; *Stoy et al.*, 2005; *Schwalm et al.*, 2010; *Dietze et al.*, 2011]. With parameter estimation conditioned on the timescale of observations during the inverse phase of the process, however, comes the necessity to generate meteorological drivers at the same timescale for use during forward projections. Previous studies have indeed shown the potential for error when mismatches are allowed between the timescales used in parameter estimation and subsequent forward deployment [*Stoy et al.*, 2005; *Richardson et al.*, 2010]. This condition has rendered the use of these models difficult for forecasting carbon cycle processes in future climate regimes and created the need to generate downscaled climate data capable of driving flux predictions [e.g., *Ueyama et al.*, 2009; *Jansson et al.*, 2008; *Grant et al.*, 2011].

[5] Here, we present an analysis in which we have confronted these challenges by using a pair of weather generator models to produce multiple realizations of future weather within a single projected climate scenario. Weather generator models have been used in numerous past studies for the purpose of downscaling projections from climate models [for review, see *Wilks and Wilby*, 1999; *Wilks*, 2012]. In this study, our interest was not to further develop the weather generator approach per se but rather to couple weather generation to an ecosystem process model to provide an improved match between the scales of assimilated flux observations and meteorological drivers for a projected future climate regime. The responses of forest metabolism to weather variables were predicted with a simple ecosystem process model (Simplified Photosynthesis and Evapotranspiration; SIPNET). By combining SIPNET with an ensemble of future weather projections, we were able to estimate multiple responses of NEE that were equally justified within the context of regional climate change. We used this approach to predict future NEE for an evergreen, subalpine forest in the Rocky Mountains of Colorado (the Niwot Ridge AmeriFlux site). This forest has been the site of numerous past studies that have focused on the relations between carbon fluxes and seasonal-to-interannual climate variation [e.g., *Monson et al.*, 2002; *Monson et al.*, 2005; *Sacks et al.*, 2007; *Moore et al.*, 2008; *Hu et al.*, 2010b]. From the form of these previously studied relations, several predictions have been generated concerning the possible responses of forest-atmosphere carbon exchanges in the face of climate change. Here, we were able to evaluate these predictions using model approaches with explicitly defined climate and weather projections for the period 2080–2099.

2. Methods and Materials

2.1. Site Description

[6] Observations of CO_2, H_2O, and energy fluxes have been made using the eddy covariance approach at the Niwot Ridge AmeriFlux Site. The site is located in the Front Range of the Rocky Mountains of Colorado (40°1′58″N; 105°32′47″W) at 3050 m elevation. The site is vegetated by a subalpine

forest dominated by three tree species: lodgepole pine (*Pinus contorta*), subalpine fir (*Abies lasiocarpa*), and Engelmann spruce (*Picea engelmannii*). The forest was logged in the early 20th century and has been allowed to aggrade since that time. The site straddles the ecotone between the pine-dominated forest to the east (downslope from the flux tower) and the spruce/fir-dominated forest to the west (upslope from the flux tower). For a more detailed description of forest structure including a treatment of spatial heterogeneity, see *Monson et al.* [2010]. Annual precipitation averages 800 mm, with approximately 65% falling as snow. The mean annual temperature is 1.5°C. For a more detailed description of the site's physical and meteorological characteristics, see *Monson et al.* [2002; 2005] and *Turnipseed et al.* [2003]. The tower is located less than 1 km from the Niwot Ridge Long Term Ecological Research (LTER) C1 climate station, where meteorological data have been collected since 1952 (http://culter.colorado.edu/NWT/).

2.2. Flux Measurements and SIPNET Modeling

[7] Turbulent flux measurements at the site have been described in detail in several previous publications [*Monson et al.*, 2002; *Turnipseed et al.*, 2002; 2003; *Yi et al.*, 2008; *Burns et al.*, 2011]. Briefly, we combine the turbulent flux for CO_2 with canopy storage to calculate half-hourly averaged values for NEE. The 30 min averaged data are filtered, removing points with inadequate turbulence (determined as the 21.5 m surface friction velocity, u*, below 0.2 m s^{-1}) or with instrument failure. All 30 min fluxes are available along with appropriate flags for gap-filled corrections and climate data (version 2011.04.20) at the Niwot Ridge AmeriFlux Web page (http://urquell.colorado.edu/data_ameriflux/).

[8] The SIPNET (Simplified Photosynthesis and Evapotranspiration) model is a simplified version of the PnET (Photosynthesis and EvapoTranspiration) model [*Aber and Federer*, 1992; *Aber et al.*, 1995; 1996]. In SIPNET, we partition ecosystem carbon into two pools: soil carbon and vegetation, the latter being further subdivided into plant "wood" and plant "leaf" carbon. We simulate transitions among these pools and their exchange with the environment as CO_2 fluxes, including those of photosynthesis, autotrophic respiration, and heterotrophic respiration. Descriptions of model logic and past efforts to validate parameter estimates have been provided in several past studies [*Braswell et al.*, 2005; *Sacks et al.*, 2006; 2007; *Moore et al.*, 2008; *Zobitz et al.*, 2008; *Hu et al.*, 2010a], and we direct the reader to those studies for a more complete assessment of model performance. Dynamics in ecosystem H_2O pools are resolved through consideration of rain and snowmelt water, and modified to account for leaf interception, canopy throughfall, soil infiltration, and drainage [*Sacks et al.*, 2006; *Moore et al.*, 2008]. Following resolution of the H_2O budget, available soil water is used to estimate evaporation and transpiration fluxes, and to constrain photosynthetic and respiratory CO_2 fluxes. The SIPNET model is driven by six meteorological variables that were taken from the Niwot Ridge AmeriFlux Web page (see web address above): air temperature at 21.5 m, soil temperature at 10 cm depth, relative humidity at 21.5 m, photosynthetically active radiation (PAR) above the canopy, wind speed at 21.5 m, and precipitation.

[9] We used the Metropolis-simulated annealing algorithm to optimize parameters governing the initial state and time evolution of SIPNET [*Metropolis et al.*, 1953]. Initial values and boundaries for the parameters were defined through a combination of literature values, best guesses, and actual measurements. We bounded each parameter within a range (a uniform "prior distribution") that is biologically or physically possible based on previous knowledge about the process, therefore eliminating solutions that violate prior knowledge. The ranges surrounding each parameter were similar to those used in past studies [*Sacks et al.*, 2006; *Moore et al.*, 2008]. Model optimization consisted of performing a quasi-random (subject to some progressive narrowing of parameter boundaries) walk through the multidimensional parameter space to find the parameter set that caused the model to generate the "best match" of projected NEE with observed NEE. We conducted the analysis across all years of available data. Here, "best match" is defined as the model output that maximizes likelihood (L) as follows:

$$L = \prod_{i=1}^{n} \frac{1}{\sqrt{2\pi}\sigma} e^{-(x_i-\mu_i)^2/2\sigma^2} \quad , \tag{1}$$

where n is the number of data points, x_i is the observed flux summed over time step i, μ_i is the modeled flux in time step i and is the error (one standard deviation) on each data point, relative to the model prediction. Our standard practice was to filter out those 30 min periods in which over 50% of the data were gap-filled, meaning that for this study, 77% of the available averaging periods across all 11 years were included. We estimated at each step of the optimization [*Hurrt and Armstrong*, 1996]. For a given model output (that is, a given set of μ_i values), the value of that maximizes L (which we denote $_e$) was determined by the following:

$$\sigma_e = \sqrt{\frac{1}{n}\sum_{i=1}^{n} (x_i - \mu_i)^2}. \tag{2}$$

[10] Due to the high density of assimilated data when observation time series are used, models such as SIPNET tend to best project NEE values near the central tendencies of the data; they tend to underestimate the frequencies of extremely high or low NEE [*Sacks et al.*, 2006; *Moore et al.*, 2008].

[11] As a starting point, we used the version of SIPNET described in *Moore et al.* [2008]. In applying the SIPNET model to the study, we used 11 years of CO_2 and H_2O flux data (1999–2009) obtained from the Niwot Ridge AmeriFlux web site referenced above. The model was conditioned on both net ecosystem exchange (NEE) and evapotranspiration (ET) obtained initially as 30 min averages, but then assimilated into the model as either 30 min, half-daily, daily, or monthly averages. We used the model data assimilation in *inverse mode* to optimize SIPNET parameter estimates, using meteorological data for the same 30 min flux periods that were assimilated into the model. Once model parameters were optimized for the 11 year observation period (1999–2009), the model was run in *forward mode* to make projections of NEE using meteorological drivers from downscaled climate data, processed through the weather generator, for a future 20 year period (2080–2099). The initial parameter set used to run SIPNET in inverse mode for the period 1999–2009 was

derived from previous studies on the same ecosystem [*Moore et al*., 2008; *Zobitz et al*., 2008]. The posterior estimates of 15 (out of 32) parameters from the 1999–2009 inverse runs were used to initialize forward runs in future climate scenarios (Table 1). Estimates of the remaining 17 parameters were fixed and derived from sources cited in *Moore et al*. [2008] or from recent field observations (Table 1). We used an initial spin-up period as previously described [*Sacks et al*., 2006], followed by the "optimization" runs. The estimated parameter set that yielded the maximum likelihood was taken to be the "most parsimonious" parameter set. We ran each optimization long enough to generate 150,000 accepted points, which requires 300,000–500,000 model iterations. We did not report standard errors retrieved for model parameters nor did we discuss patterns in those retrieved uncertainties. Discussion of these uncertainties has been covered in numerous past studies in which SIPNET was deployed to study patterns in the same flux data used here [*Sacks et al*., 2006; 2007; *Moore et al*., 2008; *Zobitz et al*., 2008; *Hu et al*., 2010a].

2.3. Modification of Soil Moisture in the SIPNET Model

[12] In analyzing past studies of the SIPNET model as applied to the Niwot Ridge AmeriFlux site, we noticed that predicted fractional soil moisture content during the summer was significantly higher than what we observed in the field. Admittedly, these are difficult numbers to compare, given that the *measurement values* were taken at a relatively shallow soil depth (integrated across the upper 15 cm) and the *modeled values* reflect processes from the entire rooted profile [*Hu et al*., 2010b]. Nonetheless, our past observations have revealed evidence of midsummer soil moisture limitations on ET and NEE [*Moore et al*., 2008; *Hu et al*., 2010b], which were not reflected in the modeled results [*Sacks et al*., 2006; 2007]. We examined this situation more closely, especially with regard to the soil moisture component of SIPNET (see details in the supporting information). A run of SIPNET conditioned on all 11 years of the flux data that we used revealed that soil moisture fraction (on a volumetric basis) never decreased below 0.5 (data not shown). Our observations, which have been made since 2006 at 10 cm depth, have revealed midsummer values that are typically below 0.25 (data not shown, but available at the Niwot Ridge AmeriFlux web site). We experimented with several different strategies to force the model to project soil moisture dynamics that were drier and closer in value to our observations. We decided upon two steps for remedy: (1) reducing the canopy aerodynamic resistance term in the model to

Table 1. Values Used to Initialize SIPNET for the Years 2080–2099[a]

Symbol	Definition	Value	Source
Initial Pool Values:			
$W_{S,0}$	Initial soil moisture content (fraction of $W_{S,c}$)	0.743	Optimization
$C_{W,0}$	Initial plant wood C content ($g\,C\,m^{-2}$)	9600	*M2008*
$C_{L,0}$	Initial leaf area index ($m^2\,m^{-2}$)	4.2	*M2008*
$C_{S,0}$	Initial soil C content (organic layer only) ($g\,C\,m^{-2}$)	16,000	*M2008*
$W_{P,0}$	Initial snow pack (cm water equivalent)	0	*M2008*
Photosynthesis/Respiration Parameters:			
A_{max}	Maximum net CO_2 assimilation rate ($nmol\,CO_2\,g^{-1}$ (leaf biomass) s^{-1})	4.627	Optimization
K_F	Foliar maintenance respiration as fraction of Amax (no units)	0.2996	Optimization
T_{min}	Minimum temperature for photosynthesis (°C)	–3.6626	Optimization
T_{opt}	Optimum temperature for photosynthesis (°C)	21.623	Optimization
$Q10_V$	Vegetation respiration Q_{10} (no units)	1.912	Optimization
T_s	Soil temperature at which photosynthesis and foliar respiration are shut down (°C)	0.0037	Optimization
K_{VPD}	Slope of VPD-photosynthesis relationship (kPa^{-1})	0.106	Optimization
$PPFD_{1/2}$	Half saturation point of PPFD-photosynthesis relationship ($mol\,m^{-2}\,d^{-1}$)	7.92	Optimization
NPP_L	Fraction of NPP allocated to leaf growth (no units)	0.455	Optimization
K_A	Wood respiration rate at 0°C ($g\,C\,g^{-1}\,C\,yr^{-1}$)	0.0102	Optimization
K_H	Soil respiration rate at 0°C and moisture-saturated soil ($g\,C\,g^{-1}\,C\,yr^{-1}$)	0.0037	Optimization
$Q10_S$	Soil respiration Q_{10} (no units)	4.826	Optimization
F_{Amax}	Average daily max photosynthesis as fraction of Amax (no units)	0.76	*M2008*
k	Canopy PAR extinction coefficient (no units)	0.5	*M2008*
K_L	Turnover rate of leaf C ($g\,C\,g^{-1}\,C\,yr^{-1}$)	0.13	*M2008*
Moisture Parameters:			
f	Fraction of soil water removable in one day (no units)	0.1546	Field obs.
K_{WUE}	VPD-water use efficiency relationship ($mg\,CO_2\,kPa\,g^{-1}$ H2O)	13.351	Optimization
$W_{S,c}$	Soil water holding capacity (cm (precipitation equivalent))	35.939	Optimization
R_d	Scalar relating aerodynamic resistance to wind speed (no units)	25	Field obs.
E	Fraction of rain immediately intercepted and evaporated (no units)	0.1	*M2008*
F	Fraction of water entering soil that goes directly to drainage (no units)	0.1	*M2008*
K_S	Snowmelt rate (cm (water equivalent) $°C^{-1}\,d^{-1}$)	0.15	*M2008*
$R_{soil,1}$	Scalar relating soil resistance to fractional soil wetness (no units)	0–16.4	*M2008*
$R_{soil,2}$	Scalar relating soil resistance to fractional soil wetness (no units)	0–8.6	*M2008*
Tree Physiological Parameters:			
SLW_C	C content of leaves on a per-area basis ($g\,C\,m^{-2}$ (leaf area))	270	*M2008*
F_C	Fractional C content of leaves ($g\,C\,g^{-1}$ (leaf biomass))	0.45	*M2008*
K_W	Turnover rate of plant wood C ($g\,C\,g^{-1}\,C\,yr^{-1}$)	0.014	*M2008*

[a]Initial parameters are either derived after assimilating 11 years of daily averaged Niwot Ridge AmeriFlux Data from 1998–2009 (as described in the text and labeled "Optimization" in the table), from analyses and observations in the field (labeled Field Obs. in the table), or from the sources cited by *Moore et al*. [2008] (labeled *M2008* in the table). Initial pool values are for 1 January 1999. VPD, vapor pressure deficit; PPFD, photosynthetic photon flux density; NPP, net primary productivity.

allow for greater rates of ET and (2) increasing daily uptake of H_2O by roots to allow greater partitioning of ET into T. Prior to taking these steps, the canopy aerodynamic resistance term in the model, which is estimated as a unitless scalar and is typically generated as a posterior parameter estimate, was shown to be forced frequently toward the high extreme of feasible values (e.g., estimated to be 1471 out of a possible upper limit of 1500 in the study of this forest by Moore *et al*. [2008]). Furthermore, the partitioning of ET to T was shown to be approximately four times lower in the model, compared to independent observations of sap flux in the same ecosystem [*Moore et al*., 2008]. When we manually forced both of these terms to fixed values and then ran the optimization of the model conditioned with observed fluxes, posterior (derived) values of the soil water content were lower and compared more closely to observed values (see supporting information). In order to achieve this result, other parameters, such as potential soil water holding capacity, water use efficiency, and certain photosynthetic parameters were adjusted in a pattern of compensation, though we have not conducted an analysis to reveal all compensatory changes and cross-sensitivities in these parameters. We used the modified version of the model, with the daily removal fraction fixed at 0.155 and the aerodynamic scalar term fixed at 25 in subsequent simulations.

2.4. The Earth System Models Used to Project Future Climate Scenarios

[13] In order to assess future climate projections for the Niwot Ridge AmeriFlux site, we used monthly averaged data generated by six well-established ESMs (Table 2) and extracted for the regional spatial domain containing the Niwot Ridge AmeriFlux site for the years 2080–2099. The six ESMs were chosen from the entire suite of models used in the fourth Assessment of the International Panel on Climate Change [*IPCC* 2007, Working Group 1], with primary consideration being whether the models included independent specification of snow versus rain. We used future CO_2 emissions scenario A1B from the IPCC Special Report on Emissions Scenarios (2000). We averaged values for two adjacent grid cells from the ESM model projections because the Niwot Ridge AmeriFlux site is located near the northern boundary of one grid cell; the two cells *together* provided more balanced spatial coverage north and south of the flux site, than considering only the cell that actually contained the site (Figure 1). The exact grid cells were defined by three east-west boundaries (1) 37.67N, −106.88W to 37.67N, −104.06W (the lower boundary of the most southern cell), (2) 40.46N, −106.88W to 40.46N, −104.06W (the middle boundary between the two cells), and (3) 43.25N, −106.88W to 43.25N, −104.06W (the upper boundary of the most northern cell) (Figure 1).

[14] The aim of our study was not to compare ESM model performance, but rather to use a broad range of models to generate a reasonable projection of future climate for our study site—thus we did not assess why each model produced differences in their projections. Rather, we used their average output as an ensemble projection of climate tendencies. We recognize that each of the six models is based on different representations of climate physics and that these differences will create uncertainty in the ultimate projections that we used. We chose not to conduct sensitivity analyses to determine the influence of these differences on our projections of ecosystem processes; a task worthy of an independent study in its own right. Rather, by averaging the projections of the models, we hoped to obtain a broad and robust perspective on future climate at this site.

[15] The modeled grids include topography that varies with elevations ranging from approximately 4000 m to approximately 1500 m. Ecosystem types within each domain include semiarid, short-grass prairie at the lowest elevations (with mean annual precipitation of 300 mm and mean annual temperatures of approximately 10°C) and alpine tundra at the highest elevations (with mean annual precipitation of approximately 800 mm and mean annual temperatures of 0°C). The ESM models do not account for these gradients and in averaging climate for the entire grid, a form of "topographic smoothing" occurs. To remove model biases and to adjust grid point climate projections to the elevation of the flux site, we applied ESM mean monthly anomalies (in terms of differences for temperature and change ratios for precipitation from a baseline period of 1980–1999) to the LTER C1 Climate Station monthly climatological means for the same baseline [*Mearns et al*., 2001]; this created an adjusted future (2080–2099) monthly time series of temperature and precipitation.

2.5. Weather Generator (WGEN) and MT-CLIM4 models

[16] In order to downscale and disaggregate the projected monthly time series from the ESMs into a daily time series, we used the Weather Generator (WGEN) model [*Richardson*, 1981; *Parlange and Katz*, 2000; *Kittel et al*., 2004]. The WGEN model was conditioned on C1 daily climate data from 1980 to 1999 to determine distributions and serial and cross-correlations of daily minimum and maximum temperature and precipitation events depending on month. WGEN was

Table 2. List of General Earth System Models (ESMs) Used in the Analysis to Provide Climate Predictions for the Years 2080–2099[a]

Model	Institution	Citation/Web Page
CSIRO-Mk3	CSIRO Atmospheric Research, Melbourne, Australia	cmar.csiro.au/e-print/open/gordon_2002a.pdf
GISS-AOM	NASA/Goddard Institute for Space Studies, New York, NY, USA	aom.giss.nasa.gov/
INM-CM3.0	Institute for Numerical Mathematics, Russian Academy of Science, Russia	*Diansky and Volodin* (2002)
MIROC3- high res MIROC3- med res	Center for Climate System Research (Univ. of Tokyo), Natl. Inst. for Environmental Studies, and Frontier Research Center for Global Change (JAMSTEC)	ccsr.u-tokyo.ac.jp/kyosei/hasumi/MIROC/tech-repo.pdf
CCSM3	National Center for Atmospheric Research (NCAR) Boulder, CO, USA	http://www.ccsm.ucar.edu

[a]CSIRO, Commonwealth Scientific and Industrial Research Organisation; AOM, Atmosphere-Ocean Model; CM, climate model; JAMSTEC, Independent Administrative Institution, Japan Agency for Marine-Earth Science and Technology; CCSM, Community Climate System Model; MIROC, Model for Interdisciplinary Research on Climate.

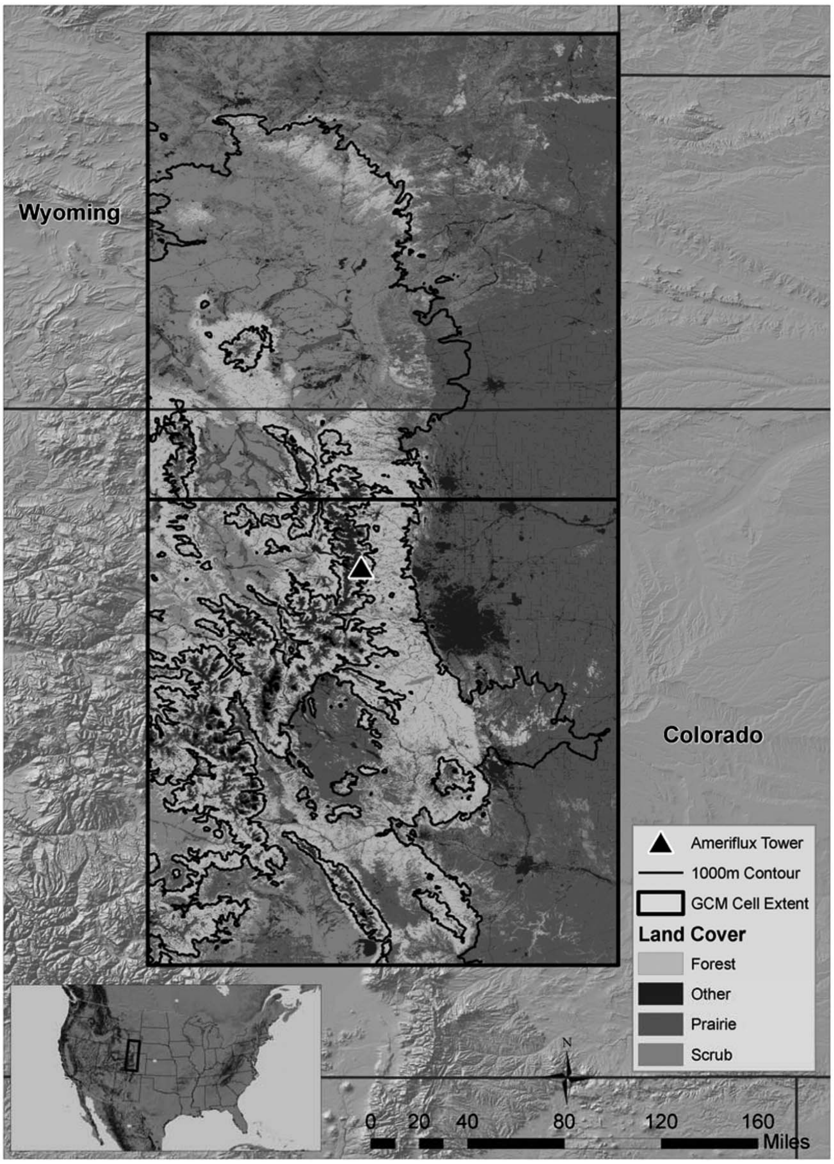

Figure 1. A map of the grid cells specified by the coordinates (37.67N, −106.875W) (37.67N, −104.0625W); (40.46N, −106.875W) (40.46N, −104.0625W); (43.25N, −106.875W) (43.25N, −104.0625W). The 1000 m isoline is shown as solid lines. The lowest elevations within both grids lie in the eastern part of the domains, with elevations between 1000 and 2000 m. The urban center of Denver, Colorado, is visible as the dark spot just east of the 2000 m isoline. The location of the Niwot Ridge AmeriFlux tower is shown with a triangle and is located at ~3000 m elevation. Major vegetation types are shown as different shades of grey. State border lines are shown in dark grey, and the grid cell boundaries are shown in black.

modified from *Kittel et al.* [2004] to have separate parameterizations for months with precipitation above and below climatological means for the conditioning period; this permitted some shifting of temperature and precipitation daily event structure in projected future climate shifts to drier or wetter states, and provides an advantage over statistical models that combine all daily records to resolve monthly probability density functions [e.g., *Hayhoe et al.*, 2008]. We viewed the conditional parameterization provided in WGEN as advantageous to predicting daily precipitation variance structure given past observations that event statistics shift under drought versus nondrought conditions [*Wilks*, 1989]—two sets of conditions that characterize the pre-monsoon and monsoon periods of summer climate at the Niwot Ridge AmeriFlux site [*Hu et al.*, 2010b]. WGEN has been evaluated in past studies using climate observations from stations across the coterminous United States during the Vegetation/Ecosystem Modeling and Analysis Project [*Kittel et al.*, 2004].

[17] WGEN uses a first-order Markov chain algorithm to predict whether a day will be wet or dry, depending on whether precipitation occurred on the previous day; then it stochastically assigns precipitation amount according to a gamma distribution of possible event sizes. Temperature

minima and maxima are stochastically generated from corresponding distributions conditioned on precipitation occurrence and as a function of temperature minimum and maximum serial trends and cross-correlations. Thus, the model creates a daily time series that manufactures the persistence of wet and dry periods, minimum and maximum temperature patterns that are conditioned on precipitation events, and it mimics the general intensity and duration of oscillating synoptic weather cells. In general, the daily series are driven by future projected monthly temperature and precipitation, but with a stochastic component. The stochastic nature of these simulations allowed us to create 10 ensemble members of WGEN dailies for the period 2080–2099. Each member is equally plausible but with slightly varying daily structure and monthly values—i.e., they have the same "target" ESM monthly mean, but they vary stochastically about that value. Daily temperature and precipitation output from WGEN was used to drive an empirical surface climate model, MT-CLIM4, to estimate daily solar radiation and humidity [*Thornton and Running*, 1999; *Thornton et al.*, 2000; *Kittel et al.*, 2004]. MT-CLIM4 uses day of the year, latitude, temperature, precipitation, elevation, and solar beam geometry to estimate solar radiation, daylight-period irradiance, vapor pressure, and relative humidity. Solar radiation and humidity are estimated using the assumptions that the diurnal temperature range at the site is a function of solar radiation transmittance and that daily minimum temperature is a function of dew point temperature [*Thornton and Running*, 1999]. In order to predict wind speed, we used a correlation between half-daily averaged wind speed and vapor pressure using data from the Niwot Ridge AmeriFlux tower instruments. While this correlation is not obvious in terms of underlying explanations, it was the best-fit correlation we obtained after testing wind speed against all other possible climate correlates, and it permitted us to estimate one unknown variable (wind speed) from a known variable (atmospheric vapor pressure) [wind speed = 0.0046 (vapor pressure) + 6.8; $r = -0.38$].

3. Results

[18] Past studies using the SIPNET model have used half-daily time steps, principally because the desired partitioning of NEE into its gross primary productivity (GPP) and ecosystem respiration (R_E) components was best justified when the model was able to assimilate the day-night contrast in NEE [*Sacks et al.*, 2006; 2007; *Moore et al.*, 2008]. These studies also showed that model performance in predicting most parameters was not improved when 30 min averaged flux data was assimilated, compared to half-daily averaged flux data; in fact, in most cases, model performance was degraded with the use of 30 min averaged data [*Sacks et al.*, 2007; *Moore et al.*, 2008]. It is possible that the poor performance of SIPNET when conditioned with 30 min data is due to inadequacies in the tower observation system, such that CO_2 that is stored in the canopy during a "calm" 30 min period is not adequately separated from that vented past the tower sensors in the subsequent "turbulent" 30 min period; thus "smearing" relations in the model between 30 min averaged NEE and specific micrometeorological drivers.

[19] In this study, we had access to daily averaged meteorological data from the downscaled climate projections using the WGEN and MT-CLIM4 models. We began the study with the a priori assumption that: given daily averaged meteorological data with which to drive the SIPNET model, we would be best served by conditioning the model on daily averaged NEE and ET observations. We found that the optimized posterior parameter values derived from the assimilation of daily averaged fluxes into SIPNET (Table 1) did not differ significantly from those retrieved in previous studies in which half-daily averaged fluxes were assimilated; at least for 4 of the 15 parameters that were allowed to vary during the optimization and represented the most relevant parameters with regard to defining carbon fluxes. For example, using daily averaged NEE and ET, we retrieved "optimized" values of 4.63 nmol CO_2 g^{-1} (leaf biomass) s^{-1} for the maximum (ecosystem) net CO_2 assimilation rate (A_{max}), 7.9 mol m^{-2} d^{-1} for the photon flux density of half-saturation for daily net CO_2 assimilation rate ($PPFD_{1/2}$), 0.004 g C g^{-1} yr^{-1} for the soil respiration rate at 0°C (K_H), and 4.83 for the Q_{10} for soil respiration (Q_{10s}). Using half-daily averaged NEE and ET for the first 7 years of the same database, *Moore et al.* [2008] retrieved "optimized" values of 4.98 nmol CO_2 g^{-1} (leaf biomass) s^{-1}, 8.29 mol m^{-2} d^{-1}, 0.003 g C g^{-1} yr^{-1}, and 4.66 for the same parameters.

[20] In Figure 2A, we have presented monthly averaged projected NEE for a single year (2003) using SIPNET with parameters conditioned on fluxes and associated

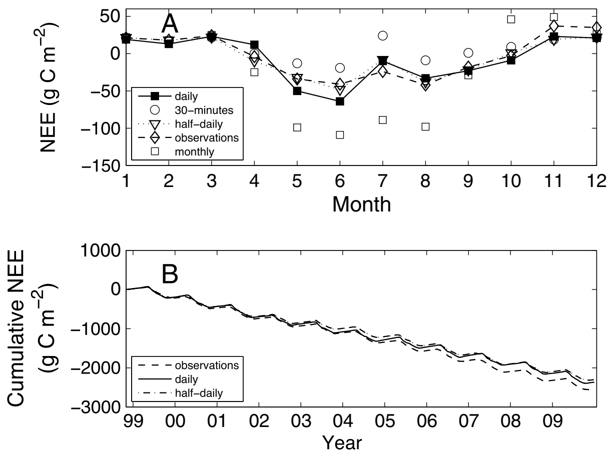

Figure 2. Comparisons between SIPNET projections of NEE conditioned on fluxes and meteorological drivers averaged at different timescales and compared to NEE observations from the 11 year Niwot Ridge AmeriFlux time series (1999–2009). (A) Monthly estimates of NEE (g C m^{-2}) over a single year (2003) from the tower flux observations (open diamonds, dashed line), and from SIPNET runs using fluxes and meteorological data (for 2003) averaged according to four different time steps: 30 min (open circles, no line), half-daily (open, inverted triangles, dotted line), daily (solid squares, solid line), and monthly (open squares, no line). (B) Cumulative NEE (g C m^{-2}) over the period 1999–2009. The lowermost dashed line was determined from tower flux observations. The solid black line represents projected NEE that was calculated using the SIPNET model with parameters conditioned on fluxes and drivers averaged at the daily time step. The grey dashed and dotted line represents projected NEE with parameters conditioned on fluxes and drivers averaged at the daily time step.

meteorological drivers averaged at 30 min, half-daily, daily, and monthly time steps, and compared to monthly averaged NEE observations. Conditioning the model with assimilated monthly averaged fluxes and meteorological drivers resulted in large overestimates of CO_2 uptake during the summer and CO_2 loss during the winter, compared to observations. Conditioning the model with fluxes and drivers averaged at the 30 min time step resulted in a substantial underestimate of net CO_2 uptake during most of the year. When conditioned with fluxes and drivers averaged at the half-daily time step, projections of NEE closely matched observations through the entire year. Finally, when conditioned with fluxes and drivers averaged at the daily time step, projections of NEE diverged from those using half-daily values in the early summer and early winter, but overall, they were quite similar.

[21] In Figure 2B, we have presented observations and modeled results of cumulative NEE across all 11 years of the assimilated flux observations, using either daily or half-daily averaged fluxes and drivers for model conditioning. In this analysis, the model performed slightly better when projecting NEE after conditioning with fluxes and drivers averaged at the daily time step (overall root mean squared error of 0.54), compared to the run with fluxes and drivers averaged at the half-daily time step (overall root mean squared error of 0.71). Overall, the model reproduced the assimilated NEE fluxes reasonably well with daily averaged fluxes and drivers, except for 2005, where model projections of net CO_2 uptake were lower than observations, and this difference continued to increase, converging with the half-daily run in 2007. The half-daily run began to diverge from observations in 2002 and continued to project lower net CO_2 uptake rates through 2009. It is noteworthy that 2002, the year that the half-daily averaged run began to diverge significantly from observations, exhibited the earliest start to the growing season in the 11 year flux record and had the driest summer recorded in the 50 year climate record for this site; whereas, 2005, the year that the daily averaged run began to diverge significantly from observations, exhibited the latest start to the growing season in the 11 year flux record and had a warmer-than-average growing season [*Hu et al.*, 2010b]. Thus, inadequacies in the representation of interactions between fluxes and meteorological drivers in the model may be amplified in unique ways during years with extreme weather patterns. When the results of Figures 2A and 2B are considered together, we conclude that our original decision to use daily averaged fluxes and drivers for the SIPNET modeling as the basis for carbon cycle forecasting was reasonable when compared to past and current studies using half-daily values.

[22] *Sacks et al.* [2007] found that there was indeed a difference in the posterior estimation of GPP and R_E when using SIPNET with half-daily versus daily averaged NEE observations. In that study, it was discovered that while the model was capable of projecting nearly equal mean monthly NEE during the growing season when conditioned on either half-daily or daily averaged fluxes, the projections of mean monthly GPP and R_E were significantly higher for the daily averaged runs. The study by *Sacks et al.* [2007] used the SIPNET model conditioned on six (1999–2004) of the same years of Niwot Ridge AmeriFlux data as was used in this study. Although it should be noted that there was a major correction applied to the Niwot Ridge flux data in 2011, rendering the Sacks et al. data set and the data set used in the current study as two different versions. Nonetheless, we found the same pattern previously recognized by *Sacks et al.* [2007], whereby the SIPNET model projected similar NEE, but greater GPP and R_E, when conditioned on daily averaged fluxes, compared to half-daily averaged fluxes (Figure 3). It is likely that the half-daily data does indeed provide greater constraint on nighttime R_E, when assimilated into the model, and thus modulates projected GPP downward to best match the observed NEE time series. Given these observations, we recognize that our retrievals of GPP and R_E from the model runs conditioned on daily averaged flux data likely represent overestimates of the true values. However, given our access to daily averaged micrometeorological drivers, and the analysis discussed in the next paragraph that shows similarity between the daily averaged and half-daily averaged NEE projections, we decided to retain the use of daily averaged NEE and ET data for model conditioning and note the potential for overestimate in the retrieved values for GPP and R_E.

[23] Considerable variation existed among projections of temperature and precipitation from the six ESM models (Figure 4A). The projected increase in mean monthly temperature ranged across 14°C during the midsummer months and 3.5°C during the midwinter months. The averaged projection from all models was approximately 10.0°C warmer than current monthly maximum midsummer temperatures, and approximately 5.3°C warmer than current monthly maximum midwinter months. Total monthly precipitation falling as rain was projected to increase up to 2.5 dm in May, the wettest month of the year (Figure 4B). Two of the models, the CSIRO-Mk3 and NCAR-CCSM3, predicted that maximum seasonal rainfall would occur in June, whereas the remainder of the models predicted May as the wettest month. Similarly, winter snowfall amounts varied across model projections, spanning a range of approximately 0.9 dm (Figure 4C). All of the models predicted that a significant fraction of future winter (December–February) precipitation would fall as rain, rather than snow (Figure 4D).

[24] In Figure 5, we compare the distribution of monthly precipitation totals measured at the Niwot Ridge AmeriFlux tower for the years 1999–2009 (Figure 5A), the seasonal precipitation patterning of the "training data" from 1980 to 1999 (Figure 5B), and a single WGEN/MT-CLIM4 run ("run 1") averaged over the years 2080–2099 (Figure 5C). Thus, data presented in Figures 5A and 5B represent observations, though from two different time series, and the data presented in Figure 5C represents modeled data from the weather generator conditioned on future climate projections from the six ESMs. Comparison of Figures 5A and 5C, which includes observed versus modeled data, respectively, shows that the combination of WGEN and MT-CLIM4 is able to realistically retrieve the seasonal distribution and daily variance in precipitation that was assimilated from the C1 meteorological observations. It is noteworthy, however, that projections for the annual distribution of precipitation in the 2080–2099 scenarios (Figure 5C) show significantly higher median amounts (1.5–2.0 times higher) during the winter months of December and January, compared to the 1980–1999 training data (Figure 5B); in this case, with the increase projected to be for predominantly rain, rather than snow. One assumption implicit in the

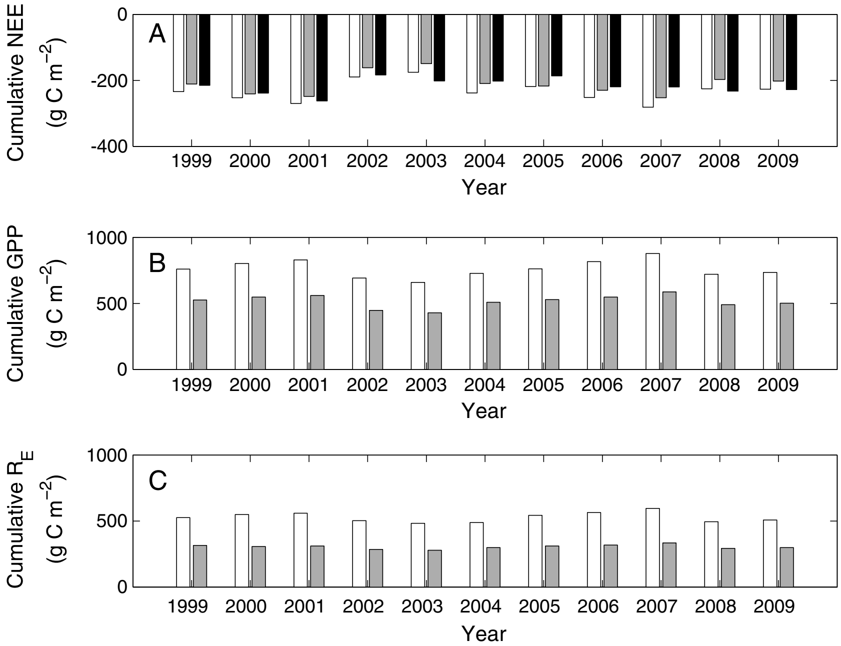

Figure 3. (A) Annual cumulative NEE for each of the 11 years used in conditioning the SIPNET model shown for runs with daily averaging of fluxes and drivers (white bars), half-daily averaging of fluxes and drivers (grey bars), and observations (black bars). (B) Annual cumulative GPP retrieved as a posterior parameter estimate for each of the 11 years used in conditioning the SIPNET model shown for runs with daily averaging of fluxes and drivers (white bars) and half-daily averaging of fluxes and drivers (grey bars). (C) Annual cumulative R_E retrieved as a posterior parameter estimate for each of the 11 years used in conditioning the SIPNET model shown for runs with daily averaging of fluxes and drivers (white bars) and half-daily averaging of fluxes and drivers (grey bars).

precipitation distribution patterns presented in Figure 5 is that the statistics driving the downscaling of monthly precipitation to daily precipitation are the same in the future projected climate for the Niwot Ridge AmeriFlux site, as they are in the climate regime during 1980–1999.

[25] There is potential for bias in our use of different time frames for the derivation of climate drivers used in the SIPNET modeling. We used weather data for the period 1980–1999 to train the WGEN and MT-CLIM4 models and generate projected meteorological drivers for the SIPNET runs in future climate scenarios. However, we used weather data for the period 1999–2009 to drive the SIPNET runs for the present climate scenario. There is potential for bias in this process if climate trends during 1980–1999 were different from those during 1999–2009. There was no evidence for such bias when comparing the seasonal distribution of precipitation for these two time series (compare Figures 5A to 55B). Considering this issue further, the most complete analysis of overall climate trends at the Niwot Ridge C1 site for the approximately five decades between 1953 and 2000 showed no significant trends in mean monthly temperature (though there was a nonsignificant springtime warming trend of 0.04°C yr^{-1}) or in precipitation (*Loesleben and Chowanski*, http://culter.colorado.edu/Climate/Mrsclimate/mcssNIWOT.pdf). Even accepting the nonsignificant trend in springtime temperature, and assuming it continued through 2009, any bias in temperature between 1980–1999 and 1999–2009, must be small (less than 0.5°C), compared to the approximately 10–14°C increase in mean monthly temperature projected for the period 2080–2099. Thus, any bias in derived NEE due to our analytical approach must also be small.

[26] We used the 10 independent runs of WGEN and MT-CLIM4 to produce the climate drivers to support 10 independent runs of SIPNET, which in turn produced projected patterns of cumulative NEE (Figure 6A). The initial parameter set used to run SIPNET was estimated from the literature or using a procedure as described previously [Table 1, and in *Moore et al.*, 2008]. It is unrealistic to assume that parameters, such as carbon pool sizes, should be the same in 2080 as in 2009. Likewise, physiological parameters such as maximum photosynthetic rate and ecosystem water-use efficiency may be different in a CO_2-enhanced future atmosphere. We made the decision to use parameters from the model runs conditioned on present-day (1999–2009) observations of NEE and ET, rather than invoke arbitrary or poorly informed assumptions about how the parameters would change in a future climate. This allowed us to directly compare present-day runs of SIPNET with future projections conditioned on meteorological drivers being the only variables.

[27] In all 10 of the projected SIPNET runs, cumulative NEE is shown to be negative in sign, indicating that the projected climate potentially fosters net ecosystem carbon uptake (Figure 6A). Interpreting these figures must be done with caution, as SIPNET outputs have never been compared against a time series as long as 20 years, and cumulative analyses will compound errors in assumptions and initial conditions. Within the context of these caveats, the 10 SIPNET runs reflect aspects of the same interannual

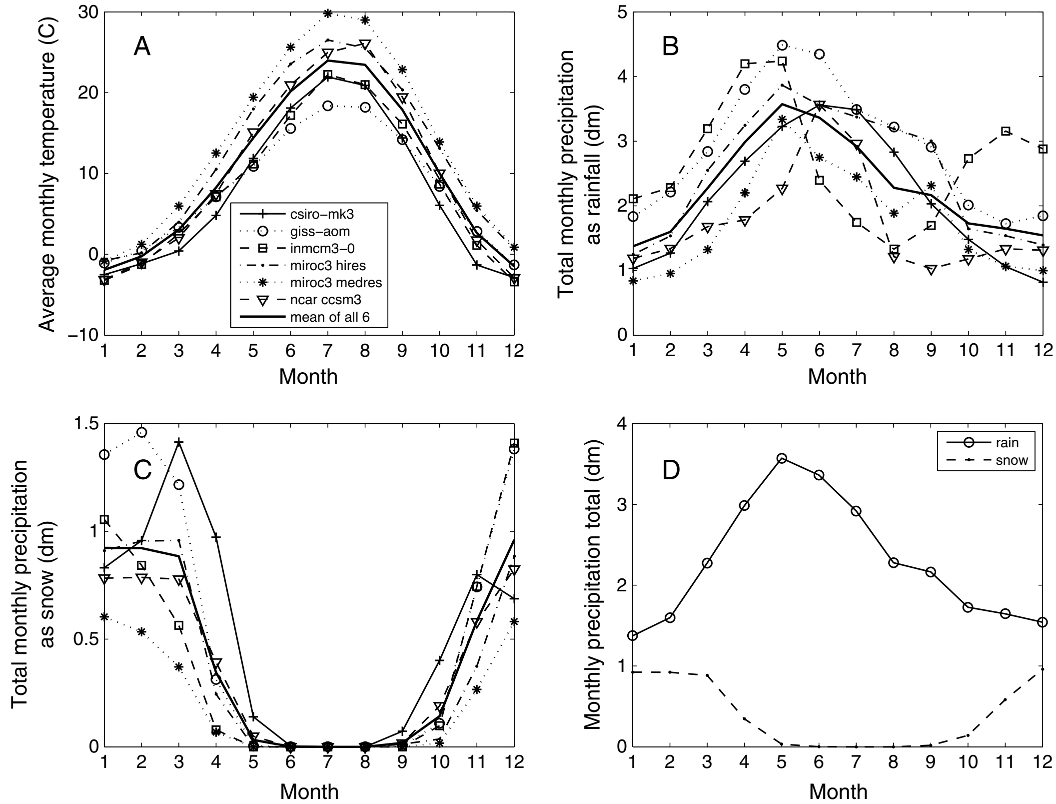

Figure 4. (A) Predicted monthly average temperature from the six ESMs. The heavy grey line shows the mean projection of all six models. (B) Predicted monthly precipitation totals falling as rain from the six ESM models. Symbols correspond to the legend presented in Figure 4A. (C) Predicted monthly precipitation falling as snow from the six ESM models. Symbols correspond to the legend presented in Figure 4A. (D) Rain and snow precipitation monthly totals averaged across all six ESMs.

variation that was assimilated into the model from the 1999–2009 eddy flux observations. A noticeable feature in 9 of the 10 runs is an attenuation of NEE in the second decade of the time series (the exception being Run 10). This attenuation is due to the effect of progressive drought during the second decade of climate data from 1980 to 1999, which was carried into the conditioning of WGEN and thus SIPNET (Figure 7). The effect of the second decade drought is especially apparent in the results of Figure 6B. Growing season decreases in both GPP and R_E were observed most clearly in 2092–2095 in runs 7–9. In essence, the lower-than-normal amounts of total annual precipitation at the C1 climate station during the period 1987–1994 created similar periods of drought in projected climate.

[28] In Figure 8, we show cumulative NEE averaged across the 10 projected SIPNET runs. Once again, a flattening in the rate of carbon uptake due to drought can be seen in the first 4 years of the second decade. In Table 3, we have summarized the change across 20 years in the future climate regime (2080–2099) for aboveground plant wood carbon, plant leaf carbon, soil carbon, and cumulative NEE predicted by the 10 SIPNET runs. The changes in these pools are given separately for the first 10 years and for the entire 20 years of the model run. All 10 runs show a similar pattern, with wood, leaf, and soil carbon pools increasing over the first 10 years, but with the leaf carbon pool actually reversing its gains and losing biomass in the second 10 years (with the exception of Run 10). The loss of biomass during the second decade is coincident with the extended drought predicted by the climate models. We note that while the general trend of increasing carbon pools in vegetation and soil is consistent with higher rates of NEE in the future climate, the SIPNET model is simple in the logic used to transfer carbon among these pools. Past studies using SIPNET at this site have revealed clear evidence of overestimation in the turnover rates of wood and soil carbon pools [*Sacks et al.*, 2006; *Zobitz et al.*, 2008]. The model is much better at predicting fluxes, such as NEE, than pools. Cumulative NEE is larger after 10 simulated years between 2080 and 2089 (average = $-4965\,\mathrm{g\,C\,m^{-2}}$) than would be expected for a decade in the current climate regime (approximately $-2100\,\mathrm{g\,C\,m^{-2}}$ was observed and modeled for the period between 1999 and 2008 using the Niwot Ridge AmeriFlux data record, see Figure 2B). This represents a projected 134 % increase in forest net CO_2 uptake due to climate change alone.

[29] The projected future climate scenarios caused a shift in the beginning of seasonal GPP and the initiation of seasonal net CO_2 uptake (i.e., negative NEE) to earlier in the year (Figure 9). This is driven by the projection of warmer winter temperatures in the future climate, and associated shifts to rain, rather than snow. In fact, monthly net CO_2 uptake is projected to begin during February or March in the future climate scenario, whereas it typically begins in April or May in the current climate regime [*Monson et al.*, 2002; 2005]. Similarly, R_E is projected

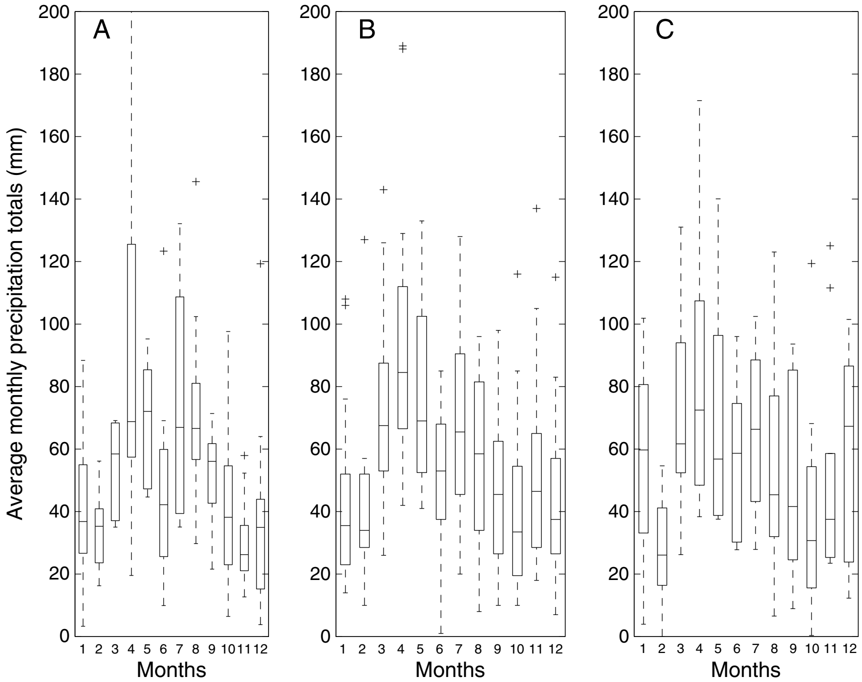

Figure 5. Boxplot comparisons of monthly precipitation total (in millimeter). In each panel, the "whiskers" show the smallest observation within 1.5 times the interquartile range from the end of the box, the bottom of the box shows the lower quartile, the central line shows the median, the top of the box shows the upper quartile, and the upper whisker shows the largest observation within 1.5 times the interquartile range from the end of the box. Points that are mathematically considered outliers are shown with a (+) symbol. (A) The distribution of monthly precipitation totals measured at the Niwot Ridge AmeriFlux tower for the years 1999–2009. (B) The seasonal precipitation patterning of the "training data" from 1980 to 1999. (C) A single WGEN run ("run 1") averaged over the years 2080–2099.

to increase earlier in the year due to warmer temperatures, though not as much as GPP, consistent with the projection of negative NEE values earlier in the year. By definition, this shift in the timing of net CO_2 uptake reflects a longer growing season. The model projections of GPP and R_E for the autumn months in the future climate do not change significantly, compared to patterns observed in the present climate. Thus, the principal effect of future climate projections on NEE are expected to occur in the early, rather than late, phases of the growing season, consistent with the analysis of *Hu et al.* [2010b] for patterns in the current climate regime. This may be due to similarities in current and projected (future) precipitation amounts and monthly distribution during the autumn months (Figure 5). We also reiterate the probability that GPP and R_E are likely overestimated in their absolute values due to the daily averaging scheme we used [*Sacks et al.*, 2007, Figure 3].

4. Discussion

[30] We pursued three principal aims. First, we developed a method of combining an ecosystem process model, conditioned on eddy flux observations, and a pair of weather generator models, conditioned on local meteorology, with site-specific climate change projections obtained from six ESMs. Second, we evaluated the potential for error between model projections and observations of NEE with regard to seasonal and multiyear dynamics given different flux and driver averaging schemes. Third, we used daily output from the weather generator models, conditioned on the future climate scenario, as the input to the ecosystem process model to investigate future responses to climate change of carbon cycling in the Niwot Ridge subalpine forest.

[31] With regard to the first aim, we were able to use state-of-the-art weather generation models to downscale monthly climate projections and produce regional-specific weather patterns at the daily scale. This allowed us to generate multiple, equally likely solutions to the problem of how *weather variation* might be averaged to produce future *mean climate*. Past studies have addressed the need to downscale the mean monthly projections of ESMs to drive ecosystem process models [e.g., *Ueyama et al.*, 2009; *Jansson et al.*, 2008; *Grant et al.*, 2011]. In fact, for the year 2011 alone, we identified 10 separate studies with the aim of downscaling monthly climate forecasts to shorter time increments for the purpose of forecasting local carbon cycling dynamics [*Ge et al.*, 2011; *Grant et al.*, 2011; *Kang et al.*, 2011; *Keenan et al.*, 2011a; 2011b; *Zhu et al.*, 2011; *Coops and Waring*, 2011; *Tao and Zhang*, 2011; *Wang et al.*, 2011; *Donmez et al.*, 2011; *Xu et al.*, 2011]. In most of these studies, the framework for downscaling involved the use of fractionalized, but constant, differences in climate between a known current time series and a projected future time series; e.g., working backward from modeled monthly climate means to bias correct a current time series, and then using those corrections to forecast a future time series at the submonthly scale. Other approaches have been used, such

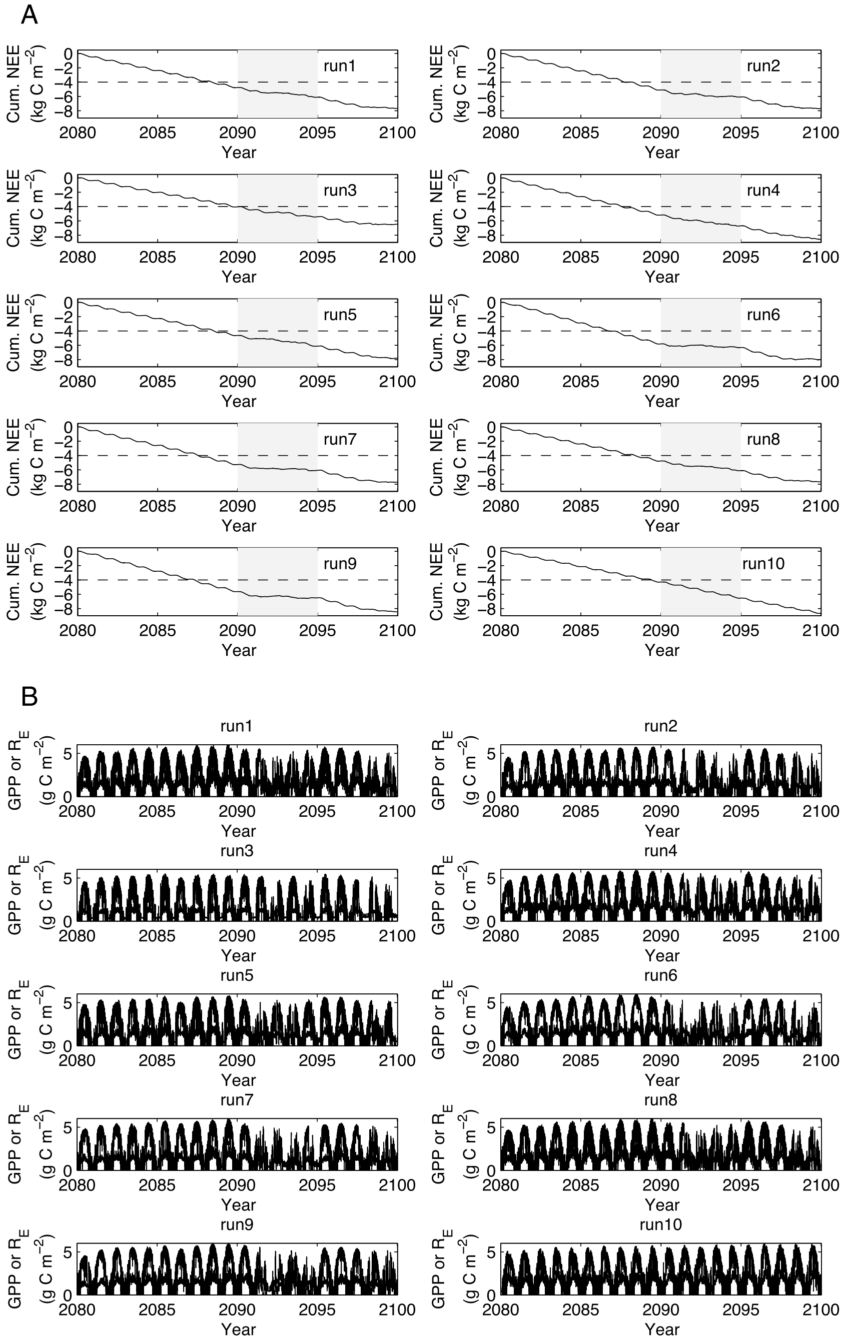

Figure 6. (A) Twenty years (2080–2099) of projected cumulative net ecosystem exchange (in kg C m^{-2}) modeled by SIPNET for 10 different model outputs of the WGEN/MT-CLIM4 model. The *x*-axes show days since the simulation starts (i.e., day 1 is 1 January 2080 and day 7305 is 31 December 2099). (B) Daily values of GPP (black) and R_E (grey) calculated by the same 10 SIPNET model runs with climate drivers from the period 2080–2099 given in g C m^{-2}.

as deploying regional climate models to downscale global climate projections, but these often include the same limitation of a monthly time step that we find in global general ESMs. Our method differs from those used in previous studies in that we took advantage of an observed daily climate record to "train" two weather generator models and thus produce daily meteorological inputs for the ecosystem process model. This approach allowed us to not only replicate natural variation in the short-term meteorological drivers that determine responses of ecosystem metabolism but they allowed us to generate multiple trajectories of daily weather that equally satisfy projected changes in mean monthly climate.

[32] In addressing the second aim of our study, we evaluated whether our approach to parsing projected climate into submonthly increments was likely to improve the accuracy

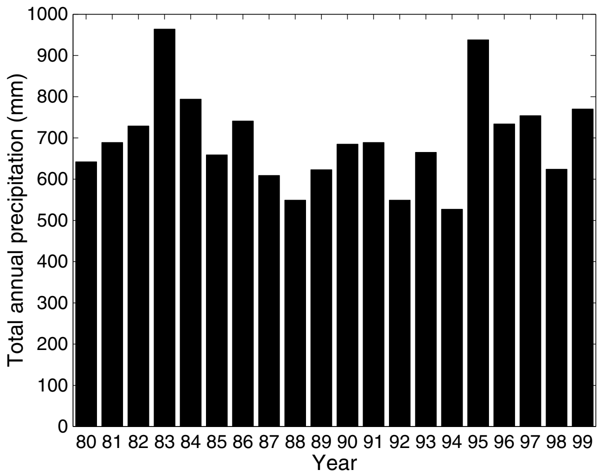

Figure 7. Two decades (1980–1999) of the WGEN model "training data" for total precipitation measured at the Niwot Ridge Long Term Ecological Research Site "C1" meteorological station. A multiyear drought is observable in the first part of the second decade. This is the drought that is likely reflected in lower NEE in the projected climate series for 2080–2099 (discussed in text). Monthly precipitation totals from these data determined the timing and frequency of "wet" and "dry" months in the WGEN model output.

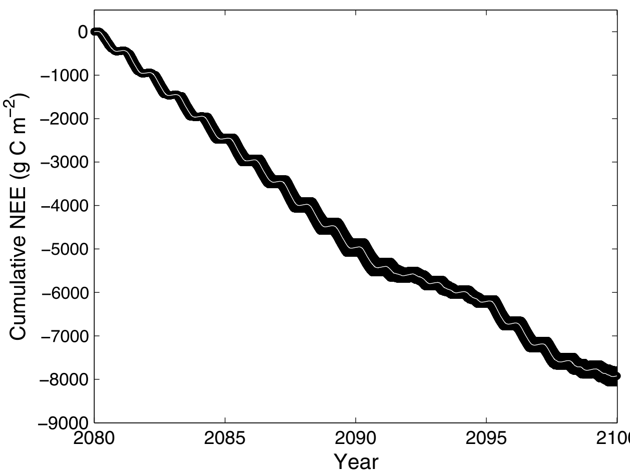

Figure 8. Cumulative NEE (grey line) averaged over the 10 SIPNET model outputs for 2080–2099 shown in Figure 5A. The *x*-axis shows days since the simulation starts, i.e. day 1 is 1 January 2080; day 7305 is 31 December 2099. The black envelope shows standard error.

of NEE projections provided by the ecosystem process model; in other words, does this approach solve the perceived problem with temporal mismatches between the daily or subdaily time step used by the ecosystem process model and the monthly time step generated from most ESM projections? In the results of Figure 2A, it is clear that running the model with monthly averaged fluxes and meteorological drivers resulted in large errors in projections of NEE. Errors due to nonlinearities and the associated averaging problems posed by Jensen's inequality [*Ruel and Ayers*, 1999], are possible causes of an overestimate of light-dependent CO_2 uptake during the day (decelerating rectangular hyperbola as photosynthetic photon flux density increases), and an underestimate of temperature-dependent CO_2 loss during the night (accelerating rectangular hyperbola as temperature increases), resulting in a predicted overestimate of net CO_2 uptake when using monthly means compared to shorter time steps [*Medvigy et al.*, 2010]. Wavelet spectral transformations have shown the daily timescale to contain the most power in predicting dynamics in the response of GPP to photosynthetic photon flux density (PPFD) and ecosystem respiration (R_E) to temperature in models conditioned on flux tower time series [*Braswell et al.*, 2005; *Stoy et al.*, 2005; *Dietze et al.*, 2011]. Less formal analyses have shown that half-daily averaging of fluxes and drivers is likely to provide improved resolution of GPP and RE as optimized parameters, when trained on observations of NEE [*Sacks et al.*, 2007]. Our results showed that daily averaging of NEE and ET prior to model conditioning provided similar retrievals of projected NEE, when compared to half-daily averaging, but overestimates of GPP and R_E. Our results demonstrate the importance of maintaining a match between the timescales used in parameter estimation and the observations used for model data error assessment [*Stoy et al.*, 2005; *Richardson et al.*, 2010].

[33] In addressing the third aim of this study, we used the coupled weather-generation and ecosystem models to forecast carbon uptake in a subalpine forest within the context of projected climate change. The six ESMs that we used for future climate projections varied significantly with regard to both air temperature and precipitation (Figure 4). All models produced projections of winter rain exceeding snow. This projection is a distinct contrast to the situation for the present climate, in which snow dominates as the winter form of precipitation, even at the lowest elevations represented in the modeled grids. The projected switch in the relative frequency of rain versus snow in the ESMs reflects the average projection for the entire spatial extent of the modeled grids. We tried to correct this "smoothing" bias to some extent by applying a change ratio (snow-to-rain) to projected changes in temperature in the C1 climate record that was used to train the weather generator models (using the baseline period 1980–1999) [*Mearns et al.*, 2001]. We have no way of assessing the effectiveness of this correction, nor of knowing whether the nonlinear form of the relation between snow/rain transition and temperature, produced new errors in the weather generation due to daily averaging. Accurate description of the snow-to-rain shift at the C1 site is crucial to understanding the influences on future NEE in this subalpine forest. The importance of this knowledge is evidenced in the large changes that projected winter warming has on the seasonal distribution of GPP and R_E (Figure 9).

[34] In a past study, we predicted that increased winter warming in future climate scenarios would cause reduced summertime GPP in the Niwot Ridge AmeriFlux forest due to reduced snowpack depth, earlier snowmelt, and reduced midsummer soil moisture [*Hu et al.*, 2010b]. This prediction was made on the basis of observations across 9 years in the AmeriFlux record reflecting current climate (1999–2007); comparing years with earlier versus later snowmelt dates. We tested this prediction in the current study to determine if the warmer winters and reduced snow

Table 3. Initial Values and Subsequent Values Over Time for Four Variables Estimated by the SIPNET Model[a]

Run	Year	Plant Wood C	Plant Leaf C	Soil C	Cumulative NEE
Initial value	2080	9,600.00	1133.60	16,000.00	0.00
1	2085	10,737.02	1565.35	17,259.55	−2827.92
	2090	11,476.16	1733.37	18,283.40	−4758.93
	2099	11,651.10	1358.74	21,381.96	−7657.80
2	2085	10,737.10	1572.25	17,379.00	−2954.35
	2090	11,483.36	1747.21	18,596.23	−5092.80
	2099	11,404.17	1319.68	21,701.85	−7691.70
3	2085	10,325.43	1377.96	17,445.81	−2415.20
	2090	10,776.40	1463.91	18,528.66	−4034.98
	2099	10,715.92	1143.47	21,334.41	−6459.80
4	2085	10,906.35	1647.74	17,338.31	−3158.41
	2090	11,662.93	1803.87	18,451.19	−5183.99
	2099	12,052.11	1476.34	21,769.79	−8564.24
5	2085	10,609.29	1504.01	17,345.22	−2724.51
	2090	11,264.46	1650.10	18,447.11	−4627.67
	2099	11,574.14	1396.27	21,551.40	−7787.81
6	2085	11,024.08	1717.94	17,463.59	−3471.60
	2090	11,903.09	1907.08	18,729.23	−5805.40
	2099	11,435.05	1349.64	21,965.81	−8016.49
7	2085	10,783.62	1591.14	17,454.02	−3094.79
	2090	11,580.87	1781.84	18,626.25	−5254.96
	2099	11,395.24	1298.22	21,752.33	−7711.79
8	2085	10,954.23	1684.82	17,434.00	−3339.05
	2090	11,797.78	1869.13	18,689.80	−5622.71
	2099	11,736.41	1412.61	22,021.10	−8436.12
9	2085	10,774.69	1593.30	17,408.69	−3042.68
	2090	11,418.32	1712.73	18,579.29	−4976.34
	2099	11,756.68	1451.74	21,762.07	−8236.49
10	2085	10,642.66	1509.08	17,151.13	−2568.87
	2090	11,248.04	1610.02	18,171.75	−4295.80
	2099	12,700.88	1769.15	20,913.74	−8649.77
Mean Pool Size Delta and Standard Error:					
	5 years	1149.45	442.76	1367.93	−2959.74
	SE	62.79	31.03	31.43	104.99
	10 years	1861.14	594.33	2510.29	−4965.36
	SE	101.05	40.95	55.74	174.97
	20 years	2042.17	263.99	5615.45	−7921.20
	SE	161.00	50.73	104.80	201.00

[a]The results of 10 runs are shown, driven by climate time series generated from 10 ensemble members of the WGEN/MT-CLIM4 model. Values are given in g C.

projected for the Niwot Ridge site would be accompanied by lower midsummer soil moisture contents and reduced midsummer GPP. We used the modified version of SIPNET with enhanced summer drawdown of soil moisture (described in Methods) to test this hypothesis. The model did not predict reduced annual NEE given the future climate projections of warm winters and reduced winter snowpack (Figure 9, Table 3). However, when compared to observations of soil moisture content, the SIPNET model performs poorly with regard to predicting early-season and late-season soil dynamics (see supporting information); the model is much better at predicting midsummer soil moisture. Given this knowledge, we focused on whether the model was predicting midsummer drought reductions in GPP during years with lower summer precipitation. The answer to this question was "probably," as the regression between July GPP and July precipitation was positive in sign ($r^2 = 0.34$) and statistically probable at the 0.06 level (data not shown). Thus, the model does seem capable of predicting reduced GPP during years with drier summers. The reason for failure of the model to predict a negative correlation between annual cumulative NEE and growing season length is likely due to the projection for increased winter rain in the future climate scenarios.

[35] Considering the overall question as to how carbon exchange in this ecosystem may change in the future, the model results revealed that warmer winter temperatures, coupled with a conversion of winter precipitation from snow to rain, will cause higher rates of CO_2 uptake by the forest. The temperature optimum for photosynthesis has been observed to be relatively low for all three dominant tree species in this ecosystem—being between 7 and 12°C—and statistical path analysis demonstrated that a slight increase in

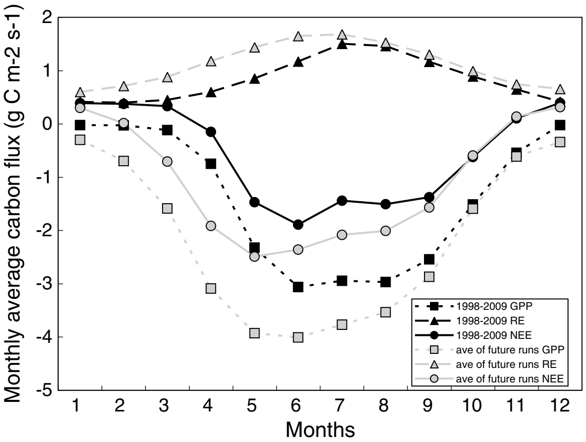

Figure 9. Monthly values of SIPNET-derived NEE, GPP, and R_E for the present climate and for the mean outputs of the 10 future climate runs as shown in Figure 6B.

temperature during the late winter and early spring is likely to increase forest net CO_2 uptake [*Huxman et al.*, 2003]. Here, the model results also showed that a slight increase in air temperature during the late winter and early spring, accompanied by higher precipitation, is likely to cause an earlier seasonal maximum in GPP. When, combined with the results of our past studies of water use in the forest, and the effects of both winter and summer drought [*Hu et al.*, 2010b], we are led to predict that winter warming will increase carbon sequestration by subalpine forests in the Western U.S., but only if liquid soil water is present. Once again, the issue as to where and to what extent snow will change to rain during the late winter months is critical to assessing future patterns of carbon cycling in this type of ecosystem.

[36] In this study, we used an ecosystem process model conditioned on a long-term record of flux observations to study the controls by weather and climate on carbon cycling in a subalpine forest ecosystem. Our approach was to: (1) use the flux observation record as a means to optimize those parameters in the model that interact with weather and control NEE, (2) deploy the optimized form of the model with meteorological inputs generated by weather generator models conditioned on synoptic variation and future climate projections, and (3) predict seasonal and interannual patterns of ecosystem-atmosphere CO_2 exchange. The advantage of this approach lies in being able to match the timescales of meteorological change with the unique physiological attributes of the subalpine forest biome, thus revealing patterns of ecophysiological and biogeochemical control at spatiotemporal scales that would not be revealed in conventional ESM modeling [*Medvigy et al.*, 2010]. Accepting these advantages, however, we also recognize that there are logistical limitations to the approach. For example, we have accounted for processes that occur during the 100 year span of projected climate change; processes such as changes in forest structure or composition, episodic disturbance (e.g., fire and insect outbreaks), or physiological acclimation. Rather, our approach focuses on changes in those processes and interactions that determine NEE within, not between, current and future climate regimes. This approach has value in elucidating controls over some of the subgrid dynamics that are averaged in ESMs, and while we have focused on only one site, our approach should be applicable to a broad range of ecosystems for which long-term flux and weather records are available.

[37] **Acknowledgments.** We are grateful to Kurt Chowanski, Mark Losleben, Lucas Zukiewicz, Kelly Matheson, Dave Millar, John Knowles, and Kirk Ranno for data collection at the Niwot Ridge C1 climate station. We thank the USDA Natural Resources Conservation Service, Colorado Snow Survey Program, for the SNOTEL network data. We thank Julie Arblaster and Gerald Meehl of the National Center for Atmospheric Research for providing ESM results for the spatial grids used in this analysis. We thank Sean Worthington for making the map in Figure 1. Diego Riveros-Iregui, John Zobitz, and Ankur Desai provided valuable discussions about the SIPNET modeling. This research was supported by the U. S. National Science Foundation (grant DEB-0743251) and the U.S. Department of Energy (grant ER-65088).

References

Aber, J. D., and C. A. Federer (1992), A generalized, lumped-parameter model of photosynthesis, evapotranspiration and net primary production in temperate and boreal forest ecosystems, *Oecologia*, *92*, 463–474.

Aber, J. D., S. V. Ollinger, C. A. Federer, P. B. Reich, M. L. Goulden, D. W. Kicklighter, J. M. Melillo, and R. G. Lathrop (1995), Predicting the effects of climate change on water yield and forest production in the northeastern United States, *Clim. Res.*, *5*, 207–222.

Aber, J. D., P. B. Reich, and M. L. Goulden (1996), Extrapolating leaf CO_2 exchange to the canopy: A generalized model of forest photosynthesis compared with measurements by eddy correlation, *Oecologia*, *106*, 257–265.

Ballantyne, A. P., C. B. Alden, J. B. Miller, P. P. Tans, and J. W. C. White (2012), Increase in observed net carbon dioxide uptake by land and oceans during the past 50 years, *Nature*, *488*, 70–73.

Booth, B. B. B., C. D. Jones, M. Collins, I. J. Totterdell, P. M. Cox, S. Sitch, C. Huntingford, R. A. Betts, G. R. Harris, and J. Lloyd (2011), High sensitivity of future global warming to land carbon cycle processes, *Environ. Res. Lett.*, *7*, Article number 024002.

Braswell, B. H., W. J. Sacks, E. Linder, and D. S. Schimel (2005), Estimating diurnal to annual ecosystem parameters by synthesis of a carbon flux model with eddy covariance net ecosystem exchange observations, *Global Change Biol.*, *11*, 335–355.

Burns, S. P., J. L. Sun, D. H. Lenschow, S. P. Oncley, B. B. Stephens, C. X. Yi, D. E. Hu, and R. K. Monson (2011), Atmospheric stability effects on wind fields and scalar mixing within and just above a subalpine forest in sloping terrain, *Boundary Layer Meteorol.*, *138*, 231–262.

Canadell, J. G., C. Le Quere, M. R. Raupach, C. B. Field, E. T. Buitenhuis, P. Ciais, T. J. Conway, N. P. Gillet, R. A. Houghton, and G. Marland (2007), Contributions to accelerating atmospheric CO_2 growth from economic activity, carbon intensity, and efficiency of natural sinks, *Proc. Natl. Acad. Sci. (USA)*, *104*, 18866–18870.

Coops, N. C., and R. H. Waring (2011), A process-based approach to estimate lodgepole pine (*Pinus contorta* Dougl.) distribution in the Pacific Northwest under climate change, *Clim. Change*, *105*, 313–328.

Diansky, N. A., and E. M. Volodin (2002), Simulation of present-day climate with a coupled atmosphere-ocean general circulation model, *Izvestiya Atmos. Ocean. Phys.*, *38*, 732–747.

Dietze, M. C., R. Vargas, A. D. Richardson, P. C. Stoy, et al. (2011), Characterizing the performance of ecosystem models across time scales: A spectral analysis of the North American carbon program site-level synthesis, *J. Geophys. Res.*, *116*, G04029, doi:10.1029/2011JG001661.

Donmez, C., S. Berberoglu, and P. J. Curran (2011), Modelling the current and future spatial distribution of NPP in a Mediterranean watershed, *Int. J. App. Earth Obs. Geoinform.*, *13*, 336–345.

Fox, A., M. Williams, A. D. Richardson, D. Cameron, J. H. Gove, T. Quaife, D. Ricciuto, M. Reichstein, E. Tomelleri, C. M. Trudinger, and M. T. Van Wijk (2009), The REFLEX project: Comparing different algorithms and implementations for the inversion of a terrestrial ecosystem model against eddy covariance data, *Agric. For. Meteorol.*, *149*, 1597–1615.

Friedlingstein, P., and I. Prentice (2010), Carbon-climate feedbacks: A review of model and observation based estimates, *Curr. Opin. Environ. Sustain.*, *2*, 251–257.

Ge, Z. M., S. Kellomaki, H. Peltola, X. Zhou, K. Y. Wang, and H. Vaisanen (2011), Impacts of changing climate on the productivity of Norway spruce dominant stands with a mixture of Scots pine and birch in relation to water availability in southern and northern Finland, *Tree Physiol.*, *31*, 323–338.

Gloor, M., J. L. Sarmiento, and N. Gruber (2010), What can be learned about carbon cycle climate feedbacks from the CO_2 airborne fraction?, *Atmos. Chem. Phys.*, *10*, 7739–7751.

Grant, R. F., E. R. Humphreys, P. M. Lafleur, and D. D. Dimitrov (2011), Ecological controls on net ecosystem productivity of a mesic arctic tundra under current and future climates, *J Geophys. Res. Biogeosciences*, *116*, Article number G01031.

Gurney, K. R., and W. J. Eckels (2011), Regional trends in terrestrial carbon exchange and their seasonal signatures, *Tellus Ser. B*, *63*, 328–339.

Hayhoe, K., C. Wake, B. Anderson, X. Z. Liang, E. Maurer, J. H. Zhu, J. Bradbury, A. DeGaetano, A. M. Stoner, and D. Wuebbles (2008), Regional climate change projections for the Northeast USA, *Mit. Adapt. Strat. Global Change*, *SI13*, 425–436.

Heimann, M., and M. Reichstein (2008), Terrestrial ecosystem carbon dynamics and climate feedbacks, *Nature*, *451*, 289–292.

Hu, J., D. J. P. Moore, D. A. Riveros-Iregui, S. P. Burns, and R. K. Monson (2010a), Modeling whole-tree carbon assimilation rate using observed transpiration rates and needle sugar carbon isotope ratios, *New Phytol.*, *185*, 1000–1015.

Hu, J., D. J. P. Moore, S. P. Burns, and R. K. Monson (2010b), Longer growing seasons lead to less carbon sequestration by a subalpine forest, *Global Change Biol.*, *16*, 771–783.

Hurrt, G. C., and R. A. Armstrong (1996), A pelagic ecosystem model calibrated with BATS data, *Deep-Sea Res. Part II-Topical Stud. Oceanog.*, *43*, 653–683.

Huxman, T. E., A. A. Turnipseed, J. P. Sparks, P. C. Harley, and R. K. Monson (2003), Temperature as a control over ecosystem CO_2 fluxes in a high-elevation, subalpine forest, *Oecologia*, *134*, 537–546.

IPCC (2007), Climate change 2007: The physical science basis, in Contribution of Working Group I to the Fourth Assessment Report of the Intergovernmental Panel on Climate Change, edited by S. Solomon, D. Qin, M. Manning, Z. Chen, M. Marquis, K. B. Averyt, M. Tignor, and H. L. Miller, Cambridge University Press, Cambridge, United Kingdom and New York, NY, USA.

Jansson, P. E., M. Svensson, D. B. Kleja, and D. Gustafsson (2008), Simulated climate change impacts on fluxes of carbon in Norway spruce ecosystems along a climatic transect in Sweden, *Biogeochemistry*, *89*, 81–94.

Kang, X. M., Y. B. Hao, C. S. Li, X. Y. Cui, J. Z. Wang, Y. C. Rui, H. S. Niu, and Y. F. Wang (2011), Modeling impacts of climate change on carbon dynamics in a steppe ecosystem in Inner Mongolia, China, *J. Soils Sed.*, *11*, 562–576.

Keenan, T. F., M. S. Carbone, M. Reichstein, and A. D. Richardson (2011a), The model-data fusion pitfall: Assuming certainty in an uncertain world, *Oecologia*, *167*, 587–597.

Keenan, T. F., E. Davidson, A. M. Moffat, W. Munger, and A. D. Richardson (2012), Using model-data fusion to interpret past trends, and quantify uncertainties in future projections, of terrestrial ecosystem carbon cycling, *Global Change Biol.*, *18*, 2555–2569.

Keenan, T. F., J. M. Serra, F. Lloret, M. Ninyerola, and S. Sabate (2011b), Predicting the future of forests in the Mediterranean under climate change, with niche- and process-based models: CO_2 matters!, *Global Change Biol.*, *17*, 565–579.

Kittel, T. G. F., et al. (2004), VEMAP phase 2 bioclimatic database. I. Gridded historical (20th century) climate for modeling ecosystem dynamics across the conterminous USA, *Clim. Res.*, *27*, 151–170.

Knorr, W. (2009), Is the airborne fraction of anthropogenic CO_2 emissions increasing?, *Geophys. Res. Lett.*, *36*, L21710.

Lawrence, D. M., P. E. Thornton, K. W. Oleson, and G. B. Bonan (2007), The partitioning of evapotranspiration into transpiration, soil evaporation, and canopy evaporation in a GCM: Impacts on land-atmosphere interaction, *J. Hydromet.*, *8*, 862–880.

Mearns, L., et al. (2001), Climate scenario development. Chapter 13, in Climate Change 2001: The Scientific Basis. Contribution of Working Group I to the Third Assessment Report of the Intergovernmental Panel on Climate Change (IPCC), edited by J. T. Houghton, Y. Ding, D. J. Griggs, M. Noguer, P. J. van der Linden, X. Dia, K. Maskell, and C. A. Johnson, Cambridge University Press.

Medvigy, D., S. C. Wofsy, J. W. Munger, and P. R. Moorcroft (2010), Responses of terrestrial ecosystems and carbon budgets to current and future environmental variability, *Proc. Natl. Acad. Sci. USA*, *107*, 8275–8280.

Meir, P., P. Cox, and J. Grace (2006), The influence of terrestrial ecosystems on climate, *Trends Ecol. Evol.*, *1*, 254–260.

Metropolis, N., A. Rosenbluth, M. N. Rosenbluth, A. H. Teller, and A. Teller (1953), Equation of state calculations by fast computing machines, *J. Chem. Phys.*, *21*, 1087–1092.

Milcu, A., M. Lukac, J. A. Subke, P. Manning, A. Heinemeyer, D. Wildman, R. Anderson, and P. Ineson (2012), Biotic carbon feedbacks in a materially closed soil-vegetation-atmosphere system, *Nat. Clim. Change*, *2*, 281–284.

Monson, R. K., A. A. Turnipseed, J. P. Sparks, P.C. Harley, L. E. Scott-Denton, K. Sparks, and T. E. Huxman (2002), Carbon sequestration in a high-elevation subalpine forest, *Global Change Biol.*, *8*, 1–20.

Monson, R. K., J. P. Sparks, T. N. Rosenstiel, L. E. Scott-Denton, T. E. Huxman, P. C. Harley, A. A. Turnipseed, S. P. Burns, B. Backlund, and J. Hu (2005), Climatic influences on net ecosystem CO_2 exchange during the transition from wintertime carbon source to springtime carbon sink in a high-elevation, subalpine forest, *Oecologia*, *146*, 130–147.

Monson, R. K., M. R. Prater, J. Hu, S. P. Burns, J. P. Sparks, K. L. Sparks, and L. E. Scott-Denton (2010), Tree species effects on ecosystem water-use efficiency in a high-elevation, subalpine forest, *Oecologia*, *162*, 491–504.

Moore, D. J. P., J. Hu, W. J. Sacks, D. S. Schimel, and R. K. Monson (2008), Estimating transpiration and the sensitivity of carbon uptake to water availability in a subalpine forest using a simple ecosystem process model informed by measured net CO_2 and H_2O fluxes, *Agric. For. Meteorol.*, *148*, 1467–1477.

Moss, R. H., et al. (2010), The next generation of scenarios for climate change research and assessment, *Nature*, *463*, 747–756.

Oleson, K. W., et al. (2008), Improvements to the community land model and their impact on the hydrological cycle, *J. Geophys. Res. – Biogeosci.*, *113*, Article number G01021.

Pan, Y. D., et al. (2011), A large and persistent carbon sink in the world's forests, *Science*, *333*, 988–993.

Parlange, M. B., and R. W. Katz (2000), An extended version of the Richardson model for simulating daily weather variables, *J. App. Meteorol.*, *39*, 610–622.

Richardson, A. D., et al. (2012), Terrestrial biosphere models need better representation of vegetation phenology: results from the North American carbon program site synthesis, *Global Change Biol.*, *18*, 566–584.

Richardson, A. D., et al. (2010), Estimating parameters of a forest ecosystem C model with measurements of stocks and fluxes as joint constraints, *Oecologia*, *164*, 25–40.

Richardson, C. W. (1981), Stochastic simulation of daily precipitation, temperature and solar radiation, *Water Res. Res.*, *17*, 182–190.

Ruel, J. J., and M. P. Ayers (1999), Jensen's inequality predicts effects of environmental variation, *Trends Ecol. Evol.*, *14*, 361–366.

Sacks, W. J., D. S. Schimel, R. K. Monson, and B. H. Braswell (2006), Model-data synthesis of diurnal and seasonal CO_2 fluxes at Niwot Ridge, Colorado, *Global Change Biol.*, *12*, 240–259.

Sacks, W. J., D. S. Schimel, and R. K. Monson (2007), Coupling between carbon cycling and climate change in a high-elevation, subalpine forest: A model-data fusion analysis, *Oecologia*, *151*, 54–68.

Schaefer, K., et al. (2012), A model-data comparison of gross primary productivity: Results from the North American carbon program site synthesis, *J. Geophys. Res.*, *117*, G03010, doi:10.1029/2012JG001960.

Schwalm, C. R., et al. (2010), A model-data intercomparison of CO_2 exchange across North America: Results from the North American carbon program site synthesis, *J. Geophys. Res.*, *115*, Article number G00H05.

Stöckli, R., D. M. Lawrence, G. Y. Niu, K. W. Oleson, P. E. Thornton, Z. L. Yang, G. B. Bonan, A. S. Denning, and S. W. Running (2008), Use of FLUXNET in the community land model development, *J. Geophys. Res. – Biogeosci.*, *113*, Article number G01025.

Stoy, P. C., G. G. Katul, M. B. S. Siqueira, J. Y. Juang, H. R. McCarthy, H. S. Kim, A. C. Oishi, and R. Oren (2005), Variability in net ecosystem exchange from hourly to inter-annual time scales at adjacent pine and hardwood forests: A wavelet analysis, *Tree Physiol.*, *25*, 887–902.

Taylor, K. E., R. J. Stouffer, and G. A. Meehl (2012), An overview of CMIP5 and the experiment design, *Bull. Amer. Met. Soc.*, *93*, 485–498.

Tao, F. L., and Z. Zhang (2011), Dynamic response of terrestrial hydrological cycles and plant water stress to climate change in China, *J. Hydrometeorol.*, *12*, 371–393.

Thornton, P. E., H. Hasenauer, and M. A. White (2000), Simultaneous estimation of daily solar radiation and humidity from observed temperature and precipitation: an application of complex terrain in Austria, *Agric. For. Meteorol.*, *104*, 255–271.

Thornton, P. E., and S. W. Running (1999), An improved algorithm for estimating incident daily solar radiation from measurements of temperature, humidity, and precipitation, *Agric. For. Meteorol.*, *93*, 211–228.

Thornton, P. E., and N. Zimmerman (2007), An improved canopy integration scheme for a land surface model with prognostic canopy structure, *J. Climate*, *20*, 3902–3923.

Turnipseed, A. A., P. D. Blanken, D. E. Anderson, and R. K. Monson (2002), Energy budget above a high-elevation subalpine forest in complex topography, *Agric. For. Meteorol.*, *110*, 177–201.

Turnipseed, A. A., D. E. Anderson, P. D. Blanken, W. M. Baugh, and R. K. Monson (2003), Airflows and turbulent flux measurements in mountainous terrain. Part 1. Canopy and local effects, *Agric. For. Meteorol.*, *119*, 1–21.

Ueyama, M., Y. Harazono, Y. Kim, and N. Tanaka (2009), Response of the carbon cycle in sub-arctic black spruce forests to climate change: Reduction of a carbon sink related to the sensitivity of heterotrophic respiration, *Agric. For. Meteorol.*, *149*, 582–602.

Wang, F. G., Y. J. Xu, and T. J. Dean (2011), Projecting climate change effects on forest net primary productivity in subtropical Louisiana, USA, *Ambio*, *40*, 506–520.

Washington, W. M., and G. A. Meehl (1984), Seasonal cycle experiment on the climate sensitivity due to a doubling of CO_2 with an atmospheric general-circulation model coupled to a simple mixed layer ocean model, *J. Geophys. Res. – Atmos.*, *89*, 9475–9503.

Wilks, D. S. (1989), Conditioning stochastic daily precipitation models on total monthly precipitation, *Water Res. Res.*, *25*, 1429–1439.

Wilks, D. S. (2012), Stochastic weather generators for climate-change downscaling, Part II: Multivariable and spatially coherent multisite downscaling, *Wiley Interdisciplin. Rev. – Clim. Change*, *3*, 267–278.

Wilks, D. S., and R. L. Wilby (1999), The weather generation game: A review of stochastic weather models, *Prog. Phys. Geog.*, *23*, 329–357.

Williams, M., et al. (2009), Improving land surface models with FLUXNET data, *Biogeosciences*, *6*, 1341–1359.

Xu, X. L., W. Liu, and G. Kiely (2011), Modeling the change in soil organic carbon of grassland in response to climate change: Effects of measured versus modelled carbon pools for initializing the Rothamsted Carbon model, *Agric. Ecosys. Environ.*, *140*, 372–381.

Yi, C. X., D. E. Anderson, A. A. Turnipseed, S. P. Burns, J. P. Sparks, D. I. Stannard, and R. K. Monson (2008), The contribution of advective fluxes to net ecosystem exchange in a high-elevation, subalpine forest, *Ecol. Appl.*, *18*, 1379–1390.

Zhao, M. S., and S. W. Running (2010), Drought-induced reduction in global terrestrial net primary production from 2000 through 2009, *Science*, *329*, 940–943.

Zhu, Q. A., H. Jiang, C. H. Peng, J. X. Liu, X. H. Wei, X. Q. Fang, S. R. Liu, G. M. Zhou, and S. Q. Yu (2011), Evaluating the effects of future climate change and elevated CO_2 on the water use efficiency in terrestrial ecosystems of China, *Ecol. Modell.*, *222*, 2414–2429.

Zobitz, J. M., D. J. P. Moore, W. J. Sacks, R. K. Monson, D. R. Bowling, and D. S. Schimel (2008), Integration of process-based soil respiration models with whole-ecosystem CO_2 measurements, *Ecosystems*, *11*, 250–269.